European Journal of Radiology 110 (2019) 163–168

Contents lists available at ScienceDirect

European Journal of Radiology

journal homepage: www.elsevier.com/locate/ejrad

Research article

Preliminary analysis: Background parenchymal 18F-FDG uptake in breast cancer patients appears to correlate with background parenchymal enhancement and to vary by distance from the index cancer

Eric Kim[a], Eralda Mema[a], Deborah Axelrod[b], Eric Sigmund[c], Sungheon Gene Kim[c], James Babb[c], Amy N Melsaether[a,*]

[a] Department of Radiology, NYU School of Medicine, New York, NY, USA
[b] Department of Surgery, Perlmutter Cancer Center, NYU School of Medicine, New York, NY, USA
[c] Bernard and Irene Schwartz Center for Biomedical Imaging, Department of Radiology, NYU School of Medicine, New York, NY, USA

ARTICLE INFO

Keywords:
Background parenchymal uptake
BPU
Breast
PET background parenchymal enhancement
BPE

ABSTRACT

Purpose: To investigate how breast parenchymal uptake (BPU) of 18F-FDG on positron emission tomography/magnetic resonance imaging (PET/MRI) in patients with breast cancer is related to background parenchymal enhancement (BPE), amount of fibroglandular tissue (FGT), and age, as well as whether BPU varies as a function of distance from the primary breast cancer.

Materials and Methods: In this institutional review board (IRB)-approved retrospective study, 40 patients (all female, ages 32–80 years, mean 52 years) gave informed consent prior to undergoing contrast enhanced breast PET/MRI from 3/2015 to 2/2018. Of the 40 patients, 6 were excluded for multicentric or bilateral cancers, 1 for current lactation and 6 because the raw data from their scans were corrupted. The remaining 27 patients (all female, ages 33 to 80 years, mean age 53 years) comprised the study population. Prone PET and contrast-enhanced MR data were acquired simultaneously on a 3-T integrated PET/ MR system. BPU was measured as SUVmax of a 1.5 cm^3 volume of interest 1) in the same quadrant of the ipsilateral breast, 5 mm from the index lesion; 2) in the opposite quadrant of the ipsilateral breast; and 3) in contralateral breast, quadrant matched to the opposite quadrant of the ipsilateral breast. The maximum standardized uptake value (SUVmax) of the index cancer was measured using a VOI that included the entire volume of the index lesion. Bleed from the primary tumor was corrected for (PET edge, MIM). FGT and BPE was assessed by 2 readers on a 4-point scale in accordance with BI-RADS lexicon. The Wilcoxon signed rank test and the Spearman rank correlation test were performed.

Results: BPU was significantly greater in the same quadrant as the breast cancer as compared with the opposite quadrant of the same breast ($p < 0.001$ for both readers) and was significantly greater in the opposite quadrant of the same breast compared to the matched quadrant of the contralateral breast ($p = 0.002$ for reader 1 and < 0.001 for reader 2). While the FGT SUVmax in the same quadrant as the cancer correlated significantly with SUVmax of the index lesion, the FGT SUVmax in the opposite quadrant of the same breast and in the matched quadrant of the contralateral breast did not. The FGT SUVmax in the contralateral breast positively correlated with the degree of BPE and negatively correlated with age, but did not show a significant correlation with the amount of FGT for either reader.

Conclusion: There appears to be an inverse correlation between metabolic activity of normal breast parenchyma and distance from the index cancer. BPU significantly correlates with BPE.

* Corresponding author at: 160 E 34th St, 3rd Floor, New York, NY 10016, USA.
E-mail addresses: Eric.Kim2@nyumc.org (E. Kim), Eralda.mema@nyumc.org (E. Mema), Deborah.axelrod@nyumc.org (D. Axelrod), PhDEric.Sigmund@nyumc.org (E. Sigmund), Gene.Kim@nyumc.org (S.G. Kim), James.Babb@nyumc.org (J. Babb), amy.melsaether@mountsinai.org (A.N. Melsaether).

https://doi.org/10.1016/j.ejrad.2018.11.031
Received 9 August 2018; Received in revised form 22 November 2018; Accepted 26 November 2018
0720-048X/ © 2018 Elsevier B.V. All rights reserved.

1. Introduction

Many types of imaging including mammography, ultrasound, and MRI, are used to screen for and to characterize breast cancers [1]. In addition to providing information about whether there is a tumor, these studies also provide background information, or information about normal breast tissue. On mammogram, the amount of fibroglandular tissue (FGT) is represented as breast density, and is categorized into 4 groups, from A, the breasts are almost entirely fatty, to D, the breasts are extremely dense [2]. This background information has been studied, and it has been shown that breast density is both a risk factor for breast cancer [3–5] and a risk factor for breast cancer going undetected by mammography [6]. On magnetic resonance imaging (MRI), background parenchymal enhancement (BPE) is the enhancement of normal FGT after intravenous contrast administration. BPE is a functional marker, reflective of perfusion and vascular permeability and, like breast density, is categorized into 4 groups, from A, minimal, to D, marked [7]. BPE has also been studied and has been shown to correlate with estrogen status, varying along with menstrual phases [8,9], decreasing with menopause [10] and in response to anti-estrogen therapies including tamoxifen [11,12], aromatase inhibitors [12–14] and oophrectomy [15,16] as well as in response to chemotherapy [17]. BPE has also been investigated as a potential risk factor for breast cancer [18–20].

Positron Emission Tomography (PET)-based imaging for breast cancer includes Positron Emission Mammography (PEM) PET/CT, and PET/MRI, which are functional and anatomic techniques that typically use fluorine-18 fluorodeoxyglucose (^{18}F-FDG) uptake to detect increased tissue metabolism via glucose. PET/MRI of the breast is an emerging tool that may provide increased specificity over MRI alone, improved nodal restaging, and also facilitates the acquisition of many PET and MRI metrics that are being investigated for their clinical utility [21]. PET/CT is a well-known whole body imaging technique commonly used in staging and restaging advanced breast cancer. PEM is a breast specific imaging modality, which uses smaller detectors with higher spatial resolution [22]. The normal FGT uptake of 18F-FDG on each of these PET imaging modalities is referred to as background parenchymal uptake (BPU).

A few studies have begun to investigate BPU to delineate its relationship with breast density, FGT and BPE. BPU obtained from PEM has been shown to correlate with breast density on mammography, but not to correlate with BPE on MRI [23]. On PET/CT, BPU has been shown to positively correlate with FGT [24] and BPE [24–26] and to vary with the menstrual cycle [25]. Thus far, the studies looking at the relationship between BPU and BPE have been limited by positioning of the breast on PET/ CT versus MRI (supine vs. prone) as well as timing of the studies in that exams are performed separately, often a few days apart. Furthermore, the effect of a primary breast cancer on BPU of the ipsilateral and contralateral breast has not been studied.

In this study, we use integrated prone breast PET/ MRI to investigate the relationship of BPU with BPE, amount of FGT and age, as well as BPU variation by location relative to a known breast cancer.

2. Materials and methods

2.1. Patient population

In this institutional review board-approved and Health Insurance Portability and Accountability Act-compliant study with written informed consent, 40 patients (all female, ages 32–80 years, mean 52 years) underwent contrast enhanced breast PET/MRI between March 2015 and February 2018 on an integrated, simultaneous PET/3 T MR system (Siemens Healthcare, Erlangen). Inclusion criteria included a biopsy-proven untreated breast cancer 2 cm or greater in maximal dimension or a biopsy-proven breast cancer of any size with at least one biopsy proven axillary nodal metastasis. Exclusion criteria included image corruption, multi-centric or bilateral breast cancer, and current lactation as additional disease sites and lactational changes compromised measurements.

2.2. Image acquisition

Each patient fasted for at least four hours prior to ^{18}F-FDG PET/MR imaging. When applicable, insulin was withheld for 6 h. Blood glucose levels were verified to be lower than 200 mg/dL (11.1 mmol/L). 555 M Bq ^{18}F-FDG was administered intravenously. Patients then rested quietly in a dark room for 45 min.

PET and MR data were acquired simultaneously with the patient in prone position and breasts in mild compression using a 3-T Biograph MR system (Siemens Healthcare, Erlangen, Germany) and a dedicated multi-channel breast coil (Noras, Wurzburg, Germany). PET data was collected for 15 min, 45–60 minutes after injection. The PET images were reconstructed for a resolution of $4.2 \times 4.2 \times 2$ mm^3 with attenuation correction using patient-specific T1-Dixon-baed attenuation correction and breast coil μ-maps. Standardized uptake value was calculated using the raw PET image values, total body mass, time from injection, and instrumental calibration factors as per standard reconstruction.

Dynamic contrast enhanced MR imaging data were acquired by using the Golden-angle RAdial Sparse Parallel (GRASP) MRI method [27]. The GRASP data were acquired using a radial stack-of-stars 3D spoiled gradient echo pulse sequence with frequency-selective fat suppression, TR/TE = 3.27/1.39,s, flip angle = 12 deg, resolution = $1.4 \times 1.4 \times 2.5$ mm^3, image matrix size = $256 \times 256 \times 80$. A total of 1497 spokes (6:29 min) were acquired to generate 5 frames of 3D images (78 s/frame using 299 spokes/frame) using the online image reconstruction provided by the manufacturer. After baseline acquisition of 78 s (29 spokes), a single dose of gadobutrol (Gadavist; Bayer Healthcare LLC, Whippany, NJ) at 0.05 mM/kg body weight was injected at 2 mL/sec, followed by saline flush with a power injector (Medrad, Indianola, Pa), while the scan continues for another 5 min 11 s (1196 spokes). This lower dose was to allow for a subsequent gadolinium injection during the whole body PET/MRI, which followed this breast exam but was not evaluated as part of this study. BPE was assessed on the 3rd frame which corresponded to approximately 90 s post-injection and was also adequate to identify the index lesion.

2.3. Image analysis

Images were sent to the picture archiving and communication system (PACS) (Intellispace, Philips, Amsterdam) and imported into MIM software (MIM, Beachwood, OH) where PET and MRI sequences were superimposed. Two breast radiologists with 8 and 1 years of experience separately localized and measured the index lesions on fused T1 post-contrast/PET images. The maximum standardized uptake value (SUVmax) of the index cancer was measured and recorded using a VOI that included the entire volume of the index lesion. SUVmax was also measured and recorded for FGT at three locations: 1) ipsilateral breast, 5 mm from the cancer in the same quadrant, 2) ipsilateral breast, opposite quadrant, and 3) contralateral breast, quadrant matched to the ipsilateral breast, using a 1.5 cm^3 volume of interest as shown in Fig. 1. An automated gradient-based contouring tool (PET Edge, MIM Software) was applied to the index cancer to correct PET bleeding artifact when obtaining SUVmax values in FGT.

In PACS, the amount of FGT was separately assessed by each radiologist on the T1-weighted pre-contrast image series on a four point scale (a. almost entirely fat, b. scattered fibroglandular tissue, c. heterogeneous fibroglandular tissue, and d. extreme fibroglandular tissue), and the amount of BPE was assessed on the first post-contrast subtracted image series on a four point scale (a. minimal, b. mild, c. moderate, and d. marked), as described in the MRI portion of the BI-RADS lexicon [7]. Patient age, menopausal status, and tumor

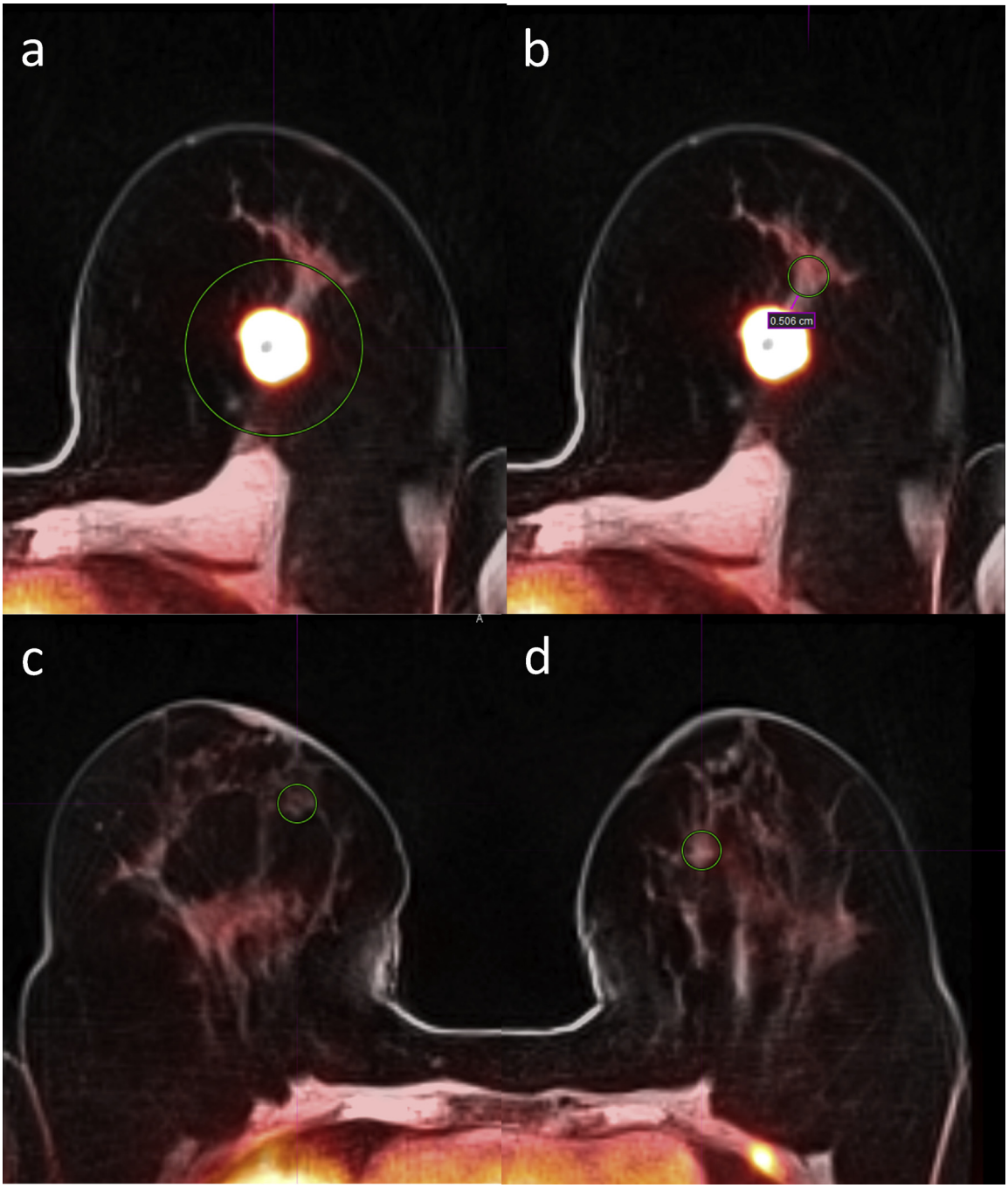

Fig. 1. Example measurements for the ^{18}F-FDG PET SUVmax values for a patient with left invasive ductal carcinoma on fused PET/MR images. (a) SUVmax = 13.24 for the target lesion. (b) SUVmax = 1.9 for the BPU in the ipsilateral breast, 5 mm from the target lesion in the same quadrant. (c) SUVmax = 0.784 for the BPU in the contralateral breast, quadrant matched to the ipsilateral breast. (d) SUVmax = 1.47 for the BPU in the ipsilateral breast, opposite quadrant. BPU values were all obtained using a 1.5 cm^3 volume of interest.

histopathology was recorded from the medical record (Epic, Verona, WI).

2.4. Statistical analysis

Inter-reader agreement in terms of the numeric SUV measures was assessed using the intra-class correlation (ICC) and in terms of the ordinal BPE and FGT measures using the linear weighted kappa coefficient. The level of agreement was interpreted as poor when the measure (M) of agreement (kappa or ICC) was less than zero, slight when $0 \leq M \leq 0.2$, fair when $0.2 < M \leq 0.4$, moderate when $0.4 < M \leq 0.6$, substantial when $0.6 < M \leq 0.8$ and almost perfect when $M > 0.8$. The Wilcoxon signed rank test was used to compare the SUV values in different locations of the same patient: ipsilateral, same quadrant vs ipsilateral, outer quadrant; ipsilateral, same quadrant vs contralateral; and ipsilateral, opposite quadrant vs contralateral. The Spearman rank correlation was used to assess the relationship of the SUV in the contralateral breast with SUVmax of lesion, BPE, FGT, and age. All statistical tests were conducted at the two-sided 5% significance level using SAS 9.3 software (SAS Institute, Cary, NC).

3. Results

Of the 40 patients, six were excluded for multicentric or bilateral

Table 1
Patient Characteristics. For Background parenchymal enhancement (BPE) and fibroglandular tissue (FGT), results are reported for each of two readers (R1 and R2).

Patient Group	Total Number
Patients	27
Age (range)	53 (33-80)
Menopausal status	
Post	14 (51.9%)
Pre	13 (48.1%)
Background Parenchymal Enhancement on MRI	
Minimal	6 (22.2%) R1, 8 (29.6%) R2
Mild	14 (51.9%) R1, 12 (44.4%) R2
Moderate	6 (22.2%) R1, 6 (22.2%) R2
Marked	1 (3.7%) R1, 1 (3.7%) R2
Fibroglandular Tissue on MRI	
Almost Entirely Fatty	6 (22.2%) R1, 5 (18.5%) R2
Scattered Fibroglandular Tissue	8 (29.6%) R1, 8(29.6%) R2
Heterogeneous Fibroglandular Tissue	7 (25.9%) R1, 8(29.6%) R2
Extreme Fibroglandular Tissue	6 (22.2%) R1, 6 (22.2%) R2
Breast Cancer Size	
2 - 4 cm	24 (88.9%)
> 4 cm	3 (11.1%)
Histopathology	
Invasive Ductal Cancer	24 (88.9%)
Invasive Lobular Cancer	1 (3.7%)
Invasive Mammary Cancer	2 (7.4%)

Table 2
The Spearman rank correlation (r) and p value for the association of SUVmax in the contralateral breast with age, BPE, FGT and SUVmax of lesion.

	Reader 1 r	Reader 1 p-value	Reader 2 r	Reader 2 p-value
Age	−0.46	0.02	−0.50	0.01
BPE	0.42	0.03	0.48	0.01
FGT	0.15	0.45	0.36	0.06

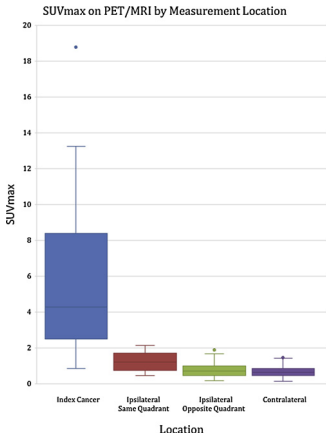

Fig. 2. SUVmax of index breast cancers and fibroglandular tissue by location. Box plots indicate median values and interquartile range (IQR). Vertical lines extend to the highest and lowest SUVmax values excluding outliers. Outliers, defined as values greater than 1.5 x IQR outside of the IQR, are indicated by circles. This figure depicts reads from Reader 1. Readers 1 and 2 had almost perfect agreement for BPU at each location with ICCs from 0.95 to 0.99.

cancers, one was excluded for current lactation and an additional six were excluded because the raw data from their scans was corrupted. The remaining twenty-seven patients (all female, ages 33 to 80 years, mean age 53 years) comprised the study population. Breast cancer type was invasive ductal cancer (IDC) in 24 patients, invasive lobular cancer (ILC) in 1 patient, and invasive mammary cancer not otherwise specified in 2 patients. There were 14 post-menopausal patients (51.9%) and 13 pre-menopausal patients (48.1%). BPE and FGT distributions are included in Table 1. Inter-reader agreement was almost perfect for both BPE (k = 0.82) and FGT (k = 0.94).

The mean SUVmax and standard deviation (SD) of the index cancers and BPU in the ipsilateral breast same quadrant, ipsilateral breast opposite quadrant, and contralateral breast are listed in Table 2. Fig. 2 shows a box plot of these values. Inter-reader agreement for BPU was almost perfect with ICC of 0.99 for BPU in the ipsilateral breast, same quadrant and ipsilateral breast, opposite quadrant and 0.95 for BPU in the contralateral breast. The BPU in the contralateral breast positively correlated with the degree of BPE and negatively correlated with age but did not show significant correlation with the amount of FGT for either reader (Table 3).

BPU decreased with increasing distance from the index lesion, from a high of 1.25 +/- 0.52 for reader 1 and 1.25 +/- 0.51 for reader 2 in the same quadrant as the index lesion to 0.63 +/- 0.38 for reader 1 and 0.62 +/- 0.4 for reader 2 in the contralateral breast, matched quadrant. BPU was significantly greater in the same quadrant as the breast cancer as compared with the opposite quadrant of the same breast for both readers ($p < 0.001$) and was significantly greater in the opposite quadrant of the same breast compared to the matched quadrant of the contralateral breast ($p = 0.002$ for reader 1 and < 0.001 for reader 2) (Table 4a). While the BPU in the same quadrant as the cancer correlated significantly with SUVmax of the index lesion, the BPU in the opposite quadrant of the same breast and in the matched quadrant of the contralateral breast did not (Table 4b).

4. Discussion

Our results show a significant moderate correlation between BPU and BPE in breast cancer patients. These results are similar to those observed by Leithner et al [24], An et al [25], and Mema et al [26], who also found positive correlations between BPU and BPE with different image acquisition techniques. These authors derived BPU from a whole body PET/CT [25,26] or breast PET/CT [24] and BPE from a separate breast MRI. Breasts are typically positioned supine in a whole-body PET/CT acquisition which compresses the breast tissue on top of itself. That our results were similar to those from studies with BPU acquired in supine position suggests that breast positioning may not have a large influence on BPU. These prior studies were somewhat limited by the timing of the PET/CT and breast MRI, as both exams were not necessarily performed on the same day, which could have weakened correlations with BPE measurements [24–26], because BPE is known to fluctuate. Like other authors, we also found that BPU inversely correlates with age [23,24,28].

Unlike Leithner et al [24], we did not see a significant positive correlation between BPU and FGT, possibly because of our small cohort. To the authors' knowledge, no other studies reported on whether FGT and BPU correlate.

Our results also show that BPU varies significantly by location relative to the known breast malignancy, with higher values nearer the index lesion and lower values in the contralateral breast. Whether this result is artifactual, related to bleed from the index lesion, or is a true finding is difficult to determine. That BPU in the same quadrant as the index lesion correlated with the SUVmax of the index lesions suggests that artifact from the tumor affects the adjacent tissue and/or that there are metabolic abnormalities in the tissues adjacent to the tumor that are not frank cancer. BPU in the quadrant opposite from the index lesion and in the contralateral breast did not correlate with the SUVmax of the index lesion, suggesting that these values are independent of the metabolic activity of the primary tumor. This pattern of uptake parallels the likelihood of breast cancer recurrence, which, in a radiation naïve breast, has been shown to be highest at the original cancer site [29]. Recurrence risk is also higher in the ipsilateral breast than in the contralateral breast [30–32]. This distribution suggests that increased metabolic activity of the non-cancerous breast tissue may reflect

Table 3
The mean, standard deviation (SD), and range of BPU (reported as SUVmax) at each location.

Location	Reader 1 SUVmax Mean ± SD	Reader 1 Range	Reader 2 SUVmax Mean ± SD	Reader 2 Range
Ipsilateral Same Quadrant	1.25 ± 0.52	0.47 - 2.13	1.25 ± 0.51	0.45-2.17
Ipsilateral Opposite Quadrant	0.82 ± 0.47	0.16 - 1.89	0.81 ± 0.47	0.16-1.71
Contralateral	0.63 ± 0.38	0.18 - 1.56	0.62 ± 0.4	0.19-1.57

Table 4a
Comparison of BPU by location using the Wilcoxon test for both readers, R1 and R2.

Comparison of BPU values between locations				p-value
Ipsilateral, Same Quadrant	R1 1.25 ± 0.52 R2 1.25 ± 0.51	Ipsilateral, Opposite Quadrant	R1 0.82 ± 0.47 R2 0.81 ± 0.47	R1 < 0.001 R2 < 0.001
Ipsilateral, Same Quadrant	R1 1.25 ± 0.52 R2 1.25 ± 0.51	Contralateral, matched quadrant	R1 0.63 ± 0.38 R2 0.62 ± 0.4	R1 < 0.001 R2 < 0.001
Ipsilateral, Opposite Quadrant	R1 0.82 ± 0.47 R2 0.81 ± 0.47	Contralateral, matched quadrant	R1 0.63 ± 0.38 R2 0.62 ± 0.4	R1 0.002 R2 < 0.001

Table 4b
The Spearman rank correlation (r) and p value for the association of SUVmax of the index lesion with SUVmax of FGT by location for each reader, R1 and R2.

	R1 r	R1 p-value	R2 r	R2 p-value
Ipsilateral, Same Quadrant	0.56	0.002	0.55	0.003
Ipsilateral, Opposite Quadrant	0.37	0.06	0.36	0.06
Contralateral	0.31	0.12	0.28	0.16

favorable host conditions for breast cancer development and growth. It would be interesting to assess whether ipsilateral BPU decreases in response to radiation therapy, which reduces local breast cancer recurrence [33], and whether bilateral BPU decreases in response to systemic chemotherapy, which may reduce both ipsilateral and contralateral breast cancer recurrences [32]. It would also be interesting to study whether, like BPE, BPU decreases with anti-estrogen therapy [11–16], and, if so, whether a decrease in BPU is associated with a decreased rate of breast cancer occurrence and could be a marker for successful chemoprevention.

Limitations of our study include that this is a retrospective study with a small sample size performed at a single institution, these results may not be generalizable to broader populations. BPE was assessed on a non-traditional T1-weighted sequence, which may have affected assessment- however, the BPE distribution was within an expected range. PET/MRI examinations were not performed during the same time of the menstrual cycle, which may have influenced BPE and BPU, although as the focus of this study was relative values of BPE, we believe any effect to be small. Lastly, the possibility of subjectivity bias may exist in qualitative assessment of BPE and manual selection of ROI to determine BPU.

In conclusion, BPU positively correlates with BPE and negatively correlates with age. Further, metabolic activity of normal breast parenchyma in breast cancer patients appears to inversely correlate with distance from the index cancer, paralleling the location pattern probability for breast cancer recurrence. Further study is warranted to investigate the role of metabolic activity in normal tissue in breast cancer development and whether BPU could be used as a modifiable imaging bio-marker for breast cancer risk.

Declarations of interest

None.

Acknowledgement

The study was supported in part by grants from the National Institute of Health (R01CA219964 and P41EB017183).

References

[1] C.H. Lee, D.D. Dershaw, D. Kopans, et al., Breast cancer screening with imaging: recommendations from the Society of Breast Imaging and the ACR on the use of mammography, breast MRI, breast ultrasound, and other technologies for the detection of clinically occult breast cancer, J. Am. Coll. Radiol. 7 (January (1)) (2010) 18–27.
[2] E.A. Sickles, C.J. D'Orsi, L.W. Bassett, et al., ACR BI-RADS® mammography, ACR BI-RADS® Atlas, Breast Imaging Reporting and Data System, American College of Radiology, Reston, VA, 2013.
[3] J.N. Wolfe, Risk for breast cancer development determined by mammographic parenchymal pattern, Cancer 37 (May (5)) (1976) 2486–2492.
[4] J.N. Wolfe, Breast patterns as an index of risk for developing breast cancer, AJR Am. J. Roentgenol. 126 (June (6)) (1976) 1130–1137.
[5] J.N. Wolfe, A.F. Saftlas, M. Salane, Mammographic parenchymal patterns and quantitative evaluation of mammographic densities: a case-control study, AJR Am. J. Roentgenol. 148 (Junuary (6)) (1987) 1087–1092.
[6] Pisano ED, Gatsonis C, Hendrick E, et al. Digital Mammographic Imaging Screening Trial (DMIST) Investigators Group. Diagnostic performance of digital versus film mammography for breast-cancer screening. N Engl J Med. 2005 Oct 27;353(17):1773-83.
[7] E.A. Morris, C.E. Comstock, C.H. Lee, et al., ACR BI-RADS® Magnetic Resonance Imaging. In: ACR BI-RADS® Atlas, Breast Imaging Reporting and Data System, American College of Radiology, Reston, VA, 2013.
[8] C.K. Kuhl, H.B. Bieling, J. Gieseke, et al., Healthy pre-menopausal breast parenchyma in dynamic contrast-enhanced MR imaging of the breast: normal contrast medium enhancement and cyclical-phase dependency, Radiology 203 (1997) 137–144.
[9] A.R. Amarosa, J. McKellop, A.P. Klautau Leite, et al., Evaluation of the kinetic properties of background parenchymal enhancement throughout the phases of the menstrual cycle, Radiology 268 (August (2)) (2013) 356–365.
[10] V. King, Y. Gu, J.B. Kaplan, J.D. Brooks, M.C. Pike, E.A. Morris, Impact of menopausal status on background parenchymal enhancement and fibroglandular tissue on breast MRI, Eur. Radiol. 22 (December (12)) (2012) 2641–2647.
[11] V. King, J. Kaplan, M.C. Pike, et al., Impact of tamoxifen on amount of fibroglandular tissue, background parenchymal enhancement, and cysts on breast magnetic resonance imaging, Breast J. 18 (6) (2012) 527–534.
[12] S. Schrading, H. Schild, M. Kühr, C. Kuhl, Effects of tamoxifen and aromatase inhibitors on breast tissue enhancement in dynamic contrast-enhanced breast MR imaging: a longitudinal intraindividual cohort study, Radiology 271 (April (1)) (2014) 45–55.
[13] V. King, S.B. Goldfarb, J.D. Brooks, et al., Effect of aromatase inhibitors on background parenchymal enhancement and amount of fibroglandular tissue at breast MR imaging, Radiology 264 (3) (2012) 670–678.
[14] N.A. Mousa, R. Elada, P. Crystal, D. Nayot, R.F. Casper, The effect of acute aromatase inhibition on breast parenchymal enhancement in magnetic resonance imaging: a prospective pilot clinical trial, Menopause 19 (4) (2012) 420–425.
[15] M.J. DeLeo 3rd, S.M. Domchek, D. Kontos, E. Conant, J. Chen, S. Weinstein, Breast MRI fibroglandular volume and parenchymal enhancement in BRCA1 and BRCA2 mutation carriers before and immediately after risk-reducing salpingo-oophorectomy, AJR Am. J. Roentgenol. 204 (3) (2015) 669–673.

[16] E.R. Price, J.D. Brooks, E.J. Watson, S.B. Brennan, E.A. Comen, E.A. Morris, The impact of bilateral salpingo-oophorectomy on breast MRI background parenchymal enhancement and fibroglandular tissue, Eur. Radiol. 24 (1) (2014) 162–168.
[17] J.H. Chen, H. Yu, M. Lin, R.S. Mehta, M.Y. Su, Background parenchymal enhancement in the contralateral normal breast of patients undergoing neoadjuvant chemotherapy measured by DCE-MRI, Magn. Reson. Imaging 31 (November (9)) (2013) 1465–1471.
[18] V. King, J.D. Brooks, J.L. Bernstein, A.S. Reiner, M.C. Pike, E.A. Morris, Background parenchymal enhancement at breast MR imaging and breast cancer risk, Radiology 260 (1) (2011) 50–60.
[19] A. Melsaether, A.C. Pujara, K. Elias, et al., Background parenchymal enhancement over exam time in patients with and without breast cancer, J. Magn. Reson. Imaging 45 (January (1)) (2017) 74–83.
[20] B.N. Dontchos, H. Rahbar, S.C. Partridge, et al., Are qualitative assessments of background parenchymal enhancement, amount of fibroglandular tissue on MR images, and mammographic density associated with breast cancer risk? Radiology 276 (August (2)) (2015) 371–380.
[21] A. Melsaether, L. Moy, Breast PET/MR imaging, Radiol. Clin. North Am. 55 (May (3)) (2017) 579–589.
[22] W.A. Berg, K.S. Madsen, K. Schilling, et al., Breast cancer: comparative effectiveness of positron emission mammography and MR imaging in presurgical planning for the ipsilateral breast, Radiology 258 (January (1)) (2011) 59–72.
[23] H.R. Koo, W.K. Moon, I.K. Chun, et al., Background ^{18}F-FDG uptake in positron emission mammography (PEM): correlation with mammographic density and background parenchymal enhancement in breast MRI, Eur. J. Radiol. 82 (October (10)) (2013) 1738–1742.
[24] D. Leithner, P.A. Baltzer, H.F. Magometschnigg, et al., Quantitative assessment of breast parenchymal uptake on 18F-FDG PET/CT: correlation with age, background parenchymal enhancement, and amount of fibroglandular tissue on MRI, J. Nucl. Med. 57 (October (10)) (2016) 1518–1522.
[25] Y.S. An, Y. Jung, J.Y. Kim, et al., Metabolic activity of normal glandular tissue on (18)F-Fluorodeoxyglucose positron emission tomography/computed tomography: correlation with menstrual cycles and parenchymal enhancements, J. Breast Cancer 20 (December (4)) (2017) 386–392.
[26] E. Mema, V.L. Mango, X. Guo, et al., Does breast MRI background parenchymal enhancement indicate metabolic activity? Qualitative and 3D quantitative computer imaging analysis, J. Magn. Reson. Imaging 47 (March (3)) (2018) 753–759.
[27] S.G. Kim, L. Feng, R. Grimm, et al., Influence of temporal regularization and radial undersampling factor on comprssed sensing reconstruction in dynamic contrast enhanced MRI of the breast, J. Magn. Reson. Imaging 43 (1) (2016) 261–269.
[28] A. Mavi, T.F. Cermik, M. Urhan, et al., The effect of age, menopausal state, and breast density on (18)F-FDG uptake in normal glandular breast tissue, J. Nucl. Med. 51 (March (3)) (2010) 347–352.
[29] E. Huang, T.A. Buchholz, F. Meric, et al., Classifying local disease recurrences after breast conservation therapy based on location and histology: new primary tumors have more favorable outcomes than true local disease recurrences, Cancer 95 (November (10)) (2002) 2059–2067.
[30] B. Fisher, S. Anderson, J. Bryant, et al., Twenty-year follow-up of a randomized trial comparing total mastectomy, lumpectomy, and lumpectomy plus irradiation for the treatment of invasive breast cancer, N. Engl. J. Med. 347 (October (16)) (2002) 1233–1241.
[31] A.K. Karam, Breast Cancer posttreatment surveillance: diagnosis and management of recurrent disease, Clin. Obstet. Gynecol. 59 (December (4)) (2016) 772–778.
[32] F. Perera, E. Yu, J. Engel, et al., Patterns of breast recurrence in a pilot study of brachytherapy confined to the lumpectomy site for early breast cancer with six years' minimum follow-up, Int. J. Radiat. Oncol. Biol. Phys. 57 (December (5)) (2003) 1239–1246.
[33] M. Clarke, R. Collins, S. Darby, et al., Early Breast Cancer trialists' Collaborative Group (EBCTCG). Effects of radiotherapy and of differences in the extent of surgery for early breast cancer on local recurrence and 15-year survival: an overview of the randomised trials, Lancet 366 (December (9503)) (2005) 2087–2106 Review.